



Article

The Influence of Solid Heat Carrier Load of Char on Pyrolysis Characteristics of Pulverized Coal in a Fluidized Bed Reactor

Xinli Li ^{1,2}, Xiaobin Qi ^{1,2,3,*} , Rui Chen ^{1,2}, Zhiping Zhu ^{1,2,4,*} and Xiaofang Wang ^{1,2,4} ¹ State Key Laboratory of Coal Conversion, Institute of Engineering Thermophysics, Chinese Academy of Sciences, Beijing 100190, China² University of Chinese Academy of Sciences, Beijing 100049, China³ Shanxi Key Laboratory of Coal Flexible Combustion and Thermal Conversion, Datong 037305, China⁴ Shanxi Engineering Research Center of Coal Clean, Efficient Combustion and Gasification, Datong 037305, China

* Correspondence: qixiaobin@iet.cn (X.Q.); zhuzhiping@iet.cn (Z.Z.)

Abstract: Pulverized coal pyrolysis based on solid heat carrier has a huge advantage in high tar yield. In this study, pyrolysis experiments on pulverized coal were conducted in a lab-scale fluidized bed reactor at 650 °C, utilizing char as the solid heat carrier. The influence of mass ratio of char to coal (RATIO) was investigated. Results show that the incorporation of solid heat carrier of char significantly enhanced the primary pyrolysis reaction in coal pyrolysis, resulting in increasing yields of tar and gas but reducing one of char. The yield of tar maximally reached 148.80–262.22% of the Gray–King analysis value at the RATIO of 14.52 g/g. As the RATIO increased, the tar contained more light component content, indicating that incorporating solid heat carriers improved the tar quality. These findings offer significant insights for the design of fluidized bed pyrolysis unit utilizing char as solid heat carrier.

Keywords: pyrolysis; fluidized bed; pulverized coal; solid heat carrier; char; pyrolysis tar



Citation: Li, X.; Qi, X.; Chen, R.; Zhu, Z.; Wang, X. The Influence of Solid Heat Carrier Load of Char on Pyrolysis Characteristics of Pulverized Coal in a Fluidized Bed Reactor. *Energies* **2024**, *17*, 2282. <https://doi.org/10.3390/en17102282>

Academic Editor: Franco Berruti

Received: 7 April 2024

Revised: 4 May 2024

Accepted: 6 May 2024

Published: 9 May 2024



Copyright: © 2024 by the authors. Licensee MDPI, Basel, Switzerland. This article is an open access article distributed under the terms and conditions of the Creative Commons Attribution (CC BY) license (<https://creativecommons.org/licenses/by/4.0/>).

1. Introduction

Pyrolysis, a widely used chemical conversion technology, enables the conversion of coal into liquid products and other chemical raw material under mild conditions [1,2]. This process is crucial for achieving efficient and clean utilization of coal [3,4]. At present, pyrolysis of lump coal (25–80 mm) has industrial-scale applications. With the advancement of mechanized coal mining technology, however, the proportion of lump coal in total quantities has been decreasing [5]. Consequently, various pyrolysis technologies with pulverized coal as raw material have been developed. With continuous understanding of pyrolysis mechanisms, it has been found that the size of coal particles plays a pivotal role in the heat and mass transfer within particles during pyrolysis [5,6] and fine particles can effectively shorten the release pathway for volatile precursors, enhancing the release of volatile products [7,8]. In order to maximize the extraction of high value-added hydrocarbon resources from coal, there exists a trend in the development of coal pyrolysis technology towards finer particle size of raw material.

Due to direct and critical impacts on pyrolysis characteristics, the process of heating pulverized coal is the core of pyrolysis technology and has always been of great concern. Among numerous heating methods, the scheme of solid heat carrier has great advantages in rapid heating [9]. For this method, common solid heat carriers include sand, ceramic balls, char, and furnace slag [10,11]. Solid heat carriers first are preheated to a predetermined temperature and then heat up coal particles at a rate of hundreds or thousands of degrees per second by mixing. Compared to the current slow pyrolysis process of lump coal, rapid thermal shock caused by solid heat carrier results in significant changes in pyrolysis performances of pulverized coal [1]. For instance, the initial temperature of gas precipitation

decreases, the yield of primary tar and gaseous hydrocarbons increases substantially, and it is easier to regulate the pyrolysis products by controlling the pyrolysis process [12]. Fushimi et al. [13] investigated pyrolysis performances of Loy Yang brown coal in a quartz glass downer pyrolyzer with silica sand as solid heat carrier. It was found that an increase in the ratio of sand/coal was beneficial for the generation of CO₂ and CO, and heavy tar was rapidly deposited on the surface of solid particles, forming cokes by polymerization. Liang et al. [14] studied the pyrolysis of Huainan bituminous coal using quartz sand as the heat carrier in an intermittent pyrolysis reactor. The results show that increasing the proportion of heat carrier can increase the yield of pyrolysis gas and inhibit the adhesion of char to the inner wall of pyrolysis reactor.

Recently, numerous technologies based on solid heat carrier have been utilized in the pyrolysis process [15–17], including rotary kiln [18], auger reactor [19], moving bed [20,21], and fluidized bed [22]. Notably, due to the features of high mass and heat transfer and strong mixing, fluidized bed reactor has been extensively employed. Such technology typically consists of two fluidized bed reactors, one used to provide solid heat carrier and the other used to achieve the pyrolysis process through fluidized mixing between pulverized coal and solid heat carrier. There exists an energy and mass balance between the two reactors, adjusted through solid circulation and reaction control. On the basis of actual needs, one reactor operates in a gasification or combustion state, accordingly providing the heat carrier with char [23,24] or ash [20,25]. Compared to ash, the heat carrier of char has advantages of significantly improving the yield of gaseous products from coal pyrolysis due to its superior surface area and pore volume [26]. Moreover, char exhibits a catalytic effect on volatile components, increasing the light oil fraction in the tar [27].

While the impact of char as heat carrier on coal pyrolysis characteristics has been extensively examined, these studies primarily focus on the variation patterns of pyrolysis products and kinetics of pyrolysis reactions. Research aiming at achieving high yield and superior quality tar remains limited and not sufficiently in-depth [28], and the findings seem not to align with practical engineering applications. For a self-sustaining pyrolysis process, the determination of mass ratio of solid heat carrier to coal is crucial for the entire process operation, such as pyrolysis temperature and circulation ration of solids, as well as coal pyrolysis behaviors including free radical fragment reaction and yield and quality of pyrolysis products [29]. Based on this, in this study, the impacts of mass ratio of char to coal (RATIO) on the pyrolysis characteristics of pulverized coal were systematically explored in a lab-scale fluidized bed pyrolyzer. The aim is to determine the optimal RATIO for efficient pyrolysis of pulverized coal and provide theoretical guidance for entire process design.

2. Experimental

2.1. Samples

Shenmu bituminous coal (SM) was used in this study. Table 1 gives the results of coal properties. Gray–King analysis indicates that the yield of tar in SM is 5.8%. The particle size of the coal, as shown in Figure 1, ranges from 0 to 0.1 mm, with a particle size for 50% cumulative volume fraction (d_{50}) of 71.58 μm .

Table 1. Ultimate and Proximate analysis and Gray–King analysis of SM and SMC.

Sample	Ultimate Analysis (% ad)					Proximate Analysis (% ad)				Gray–King Analysis (% ad)	
	C	H	O ^a	N	S	M	V	FC	A	Tar Yield ($Y_{G-K, \text{tar}}$)	
SM	70.30	4.47	13.00	0.81	0.40	4.45	29.43	59.55	6.57	5.60	
SMC	70.64	0.88	4.15	0.60	0.31	7.35	7.48	76.24	8.93	Not detected	

^a Calculated by difference; M—moisture; V—volatile matter; FC—fixed carbon; A—ash; ad—air dry basis.

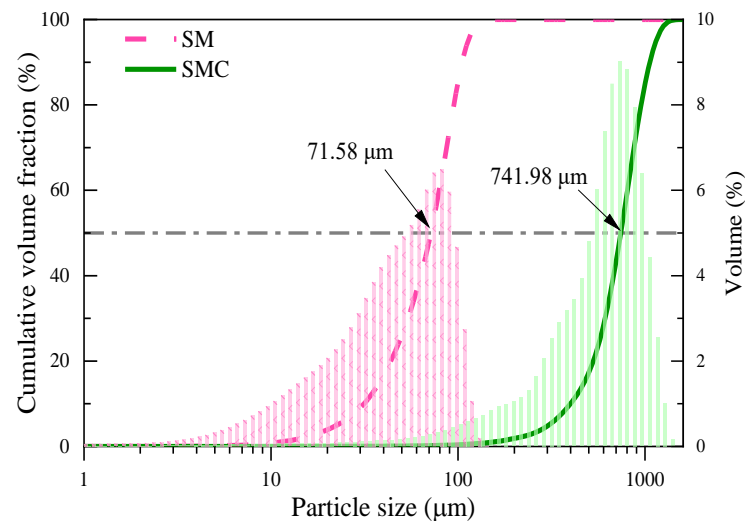


Figure 1. Particle size distribution of SM and SMC.

The solid heat carrier of char employed was prepared from SM by pyrolysis at 700 °C for 4 h, named SMC hereafter. For such char, it is believed that no tar will be generated at pyrolysis temperatures below 700 °C. Before the experiments, the SMC was sieved to a particle size range of 0.5–1.0 mm, and the particle size of d_{50} was 741.98 μm . Table 1 and Figure 1 show corresponding property results of SMC.

2.2. Experimental Apparatus and Procedure

The schematic diagram of pyrolysis apparatus is illustrated in Figure 2. The reactor, composed of stainless steel, has an inner diameter of 74 mm and a height of 530 mm. An integrated metal filter with a pore size of 2 μm is installed at the upper part of the reactor, preventing the escape of fine solid particles from affecting subsequent gas and tar sampling. One K-type thermocouple is positioned above the air distribution plate to monitor the temperature of dense phase. Additionally, a pressure sensor is employed to oversee the pressure inside the reactor. The pulverized coal is loaded to the reactor bottom through a conveying pipe under the action of sowing coal wind of N_2 . One 4 L/min N_2 flow is introduced into the reactor from the bottom, maintaining the fluidization state of solids inside the reactor. Gas flows are regulated by mass flow meters with an accuracy of 1%.

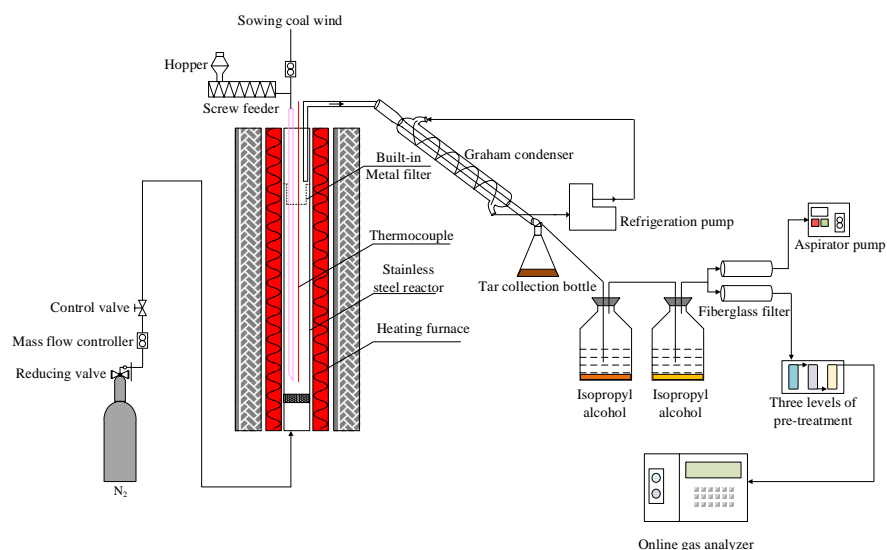


Figure 2. The schematic diagram of the SM pyrolysis experimental apparatus.

Before feeding the pulverized coal, the solid heat carrier of SMC was placed into the reactor and preheated by the heating furnace to 650 °C, the optimal temperature for maximum tar yield [27]. Such a design regarding the temperature of SMC would avoid the secondary cracking of tar due to higher temperature, as well as the release of volatiles from the solid heat carrier of SMC, interfering the results regarding the tar yield and pyrolysis gas composition. Once fed into the reactor, the pulverized coal would be rapidly heated by solid heat carrier, triggering a fast pyrolysis process. For collecting tar, the pyrolysis gas discharged from the reactor would successively undergo the processes of low-temperature cooling by refrigeration pump (−15 °C), two-stage extraction by isopropanol solution, and filtration by fiberglass, as illustrated by Figure 1. Accordingly, the tar produced was distributed in the cone-shaped collection bottle, isopropanol solution, and fiberglass filter. Following this, the gas free of tar was detected by an online gas analyzer for gas composition. When the concentration of combustible gas was lower than 5% and almost no longer changed, the pyrolysis reaction was considered finished. At this time, the experiment was terminated by turning off the heating furnace and gas flow. In this study, only the factor of the mass ratio of SMC to SM (RATIO) was investigated.

2.3. Sample Characterization

A gas chromatography mass spectrometer (GC-MS, Agilent 6890A GC, Agilent 5375 MS, Agilent Company, Santa Clara, CA, USA) was employed to detect the primary composition and structure of organic compounds in tar samples. The instrument was set to the conditions of the solvent delay time of 3 min, the ratio of the injector to the detector of 50:1, the ion source temperature of 200 °C, and the mass-to-charge ratio m/z ranging from 50–550. During the detection, the tar sample was heated at a rate of 6 °C/min to 280 °C, at which it was maintained for 10 min, using helium as the carrier gas. The peak area integral method was adopted to quantify the high concentration compounds typically found in tar. Each peak in the chromatogram represents a specific substance, determined by comparing with standard spectra of compounds in the NIST database.

To obtain the fraction composition of tar, the gas chromatographic simulation distillation experiment was conducted using the 7890A GC manufactured by Agilent Company (Santa Clara, CA, USA). The analysis method was according to the standard of ASTM D2887-01a [30] and SH/T 0558-95 [31].

The pyrolyzed char was characterized by N₂ physical adsorption test using a physical adsorption analyzer (Autosorb-IQ, Quantachrome Instrument, Boynton Beach, Florida, USA). Prior to the test, all samples underwent a drying and degassing process at 100 °C for 12 h. According to the test data, the microscopic morphology of char was obtained. The specific surface area (S_{BET}) was determined through the multi-point BET method; the total pore volume (V_{TOT}) was derived from the equilibrium adsorption capacity at the ratio P/P_0 of ~1.00; and the pore size distribution was computed using the BJH method.

The surface functional groups of char were examined using a Fourier transform infrared spectrometer (FT-IR, IR Affinity-1S, Kyoto, Japan). Before the examination, the char was subjected to drying at a temperature of 105 °C for 12 h to eliminate external water. In the tablet pressing, the mass ratio of KBr to char was approximately 100:1. The spectra from 4000 to 400 cm^{−1} were recorded with a resolution of 4 cm^{−1}.

2.4. Data Processing

According to the concentration of pyrolysis gas component measured by the online gas analyzer and assuming that no N₂ is generated in the pyrolysis, the volume yield of pyrolysis gas component i ($y_{g,i}$, L/g), the volume of pyrolysis gas component produced per unit mass the SM fed, can be calculated by N₂ balance, as follows.

$$y_{g,i} = \frac{Q_{\text{N}_2} \times \int_0^t \frac{v_{i,t}}{v_{\text{N}_2,t}} dt}{m_{\text{coal}}} \quad (1)$$

where i represents CO, CO₂, CH₄, H₂, and C_nH_m (referring to the sum of C₂H₄, C₂H₆, C₃H₆, and C₃H₈); Q_{N_2} is the flow rate of N₂ introduced, L/min; t is the time spent on the pyrolysis experiment, min; $v_{i,t}$ is the volume fraction of pyrolysis gas component i at the t minutes of pyrolysis experiment, %; $v_{N_2,t}$ is the volume fraction of N₂ at the t minutes of pyrolysis experiment, %; m_{coal} is the mass of SM used, g.

The yield of pyrolysis gas (Y_g , %), the mass percentage of pyrolysis gas produced to the SM fed, can be calculated via Equation (2).

$$Y_g = \frac{Q_{N_2} \times \int_0^t \frac{v_{g,t} \times MW_{g,t}}{v_{N_2,t}} dt}{22.4 \times m_{\text{coal}}} \times 100\% \quad (2)$$

where $MW_{g,t}$ is the average molar mass of dry pyrolysis gas, g/mol.

The yield of char (Y_{char} , %), the mass percentage of char produced to the SM fed, can be calculated by the following equation.

$$Y_{\text{char}} = \frac{m_{\text{char}}}{m_{\text{coal}}} \times 100\% \quad (3)$$

where m_{char} is the mass of char produced, g. The m_{char} can be determined by subtracting the mass of solid heat carrier from the total one of solids remaining in the reactor after the experiment.

The yield of tar (Y_{tar} , %), the mass percentage of tar collected to the SM fed, can be calculated as follows.

$$Y_{\text{tar}} = \frac{m_{\text{tar}}}{m_{\text{coal}}} \times 100\% \quad (4)$$

where m_{tar} is the mass of tar collected during the pyrolysis process, g.

3. Results and Discussion

3.1. Pyrolysis Process of SMC

As mentioned in Section 2.1, the solid heat carrier of SMC was prepared at 700 °C. In theory, no tar would be released at the pyrolysis temperature of 650 °C. However, the unexpected result that a small amount of tar might be produced from the solid heat carrier cannot be ruled out in the experiments. In order to accurately evaluate the interference of solid heat carrier on the yield of tar under experimental conditions, a blank experiment of SMC was conducted without SM. According to the results of blank experiment, the tar yield of SMC was found to be 0.27%. Consequently, in the spirit of rigor, the tar produced from SMC should be considered despite being very low.

3.2. Products Distribution

The distribution of pyrolysis products is depicted in Figure 3. As evidenced by the yield distribution diagram, without the solid heat carrier, the yields of char, tar, and gas amount to 58.35%, 5.10% (91.05% of the Gray–King analysis yield), and 4.19%, respectively. It is evident that the addition of solid heat carrier significantly elevates the tar yield, reaching a maximum value of 14.68% at the RATIO of 25.32 g/g (262.22% of the Gray–King analysis yield). This is because a large number of heat carriers conduct rapid heat exchange with pulverized coal, which accelerates the primary devolatilization reaction of pulverized coal and promotes the formation of volatiles, thereby increasing the tar yield. According to the results of blank experiment, however, this value incorporates the tar produced from the solid heat carrier of SMC. Deducting this portion of tar from the total yield, the maximum tar yield reduces to 8.33% (148.80% of the Gray–King analysis ratio), which is achieved at the RATIO of 14.52 g/g. In theory, under an optimal RATIO, the maximum tar yield ranges between 148.80% and 262.22% of the Gray–King analysis yield. Furthermore, at a RATIO below 9.67 g/g, it is observed that a higher RATIO results in a decreasing char yield but an increasing gas yield. This may be due to the intensification of primary pyrolysis reaction under the rapid heating of solid heat carrier [32]. However, when the RATIO surpasses

9.67 g/g, the char yield slightly rebounds with the increasing RATIO. In this case, besides intensification of primary pyrolysis reaction, the catalytic effect of this solid heat carrier on the secondary reaction of volatile matter released should be considered. This catalytic effect will enhance the disproportionation of tar released (especially heavy tar), generating smaller molecules of gas and larger molecules of coke [33]. Therefore, it is inferred that the solid heat carrier can regulate the pyrolysis reaction through thermal and catalytic effects.

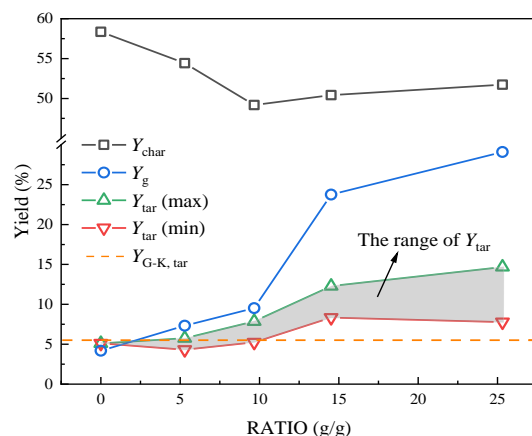


Figure 3. The effect of RATIO on product yields.

Figure 4 shows the variations in the volume yield of pyrolysis gas component by RATIO. It is evident that the pyrolysis gas mainly includes CH_4 , CO_2 , C_nH_m , H_2 , and CO . All yields of these components basically show an increasing trend with RATIO, contributing to the rise of pyrolysis gas yield. At a RATIO below 9.67 g/g, these yields follow the order of CO , H_2 , CH_4 , CO_2 , and C_nH_m (from high to low), and the yield of C_nH_m fluctuates without obviously increasing. When the RATIO is above 9.67 g/g, the yield of H_2 exceeds that of CO , becoming the highest, and the yield of C_nH_m shows a clear upward trend. Continuing to increase the RATIO actually reduces the yield of CO_2 . These results indicate the important role of RATIO in regulating the pyrolysis gas components, especially in the range of 9.67–14.52 g/g. In this range, both the thermal and catalytic effects of the solid heat carrier promote an increase in pyrolysis gas component yield. Furthermore, C_nH_m is primarily produced by the demethylation or ethylation of methyl ether bridges, aromatic side chains, and chain hydrocarbons in tar. According to the increasing trend of C_nH_m yield with RATIO, it can be inferred that the catalytic effect of the solid heat carrier gradually intensifies the secondary pyrolysis reaction when the RATIO is above 9.67 g/g.

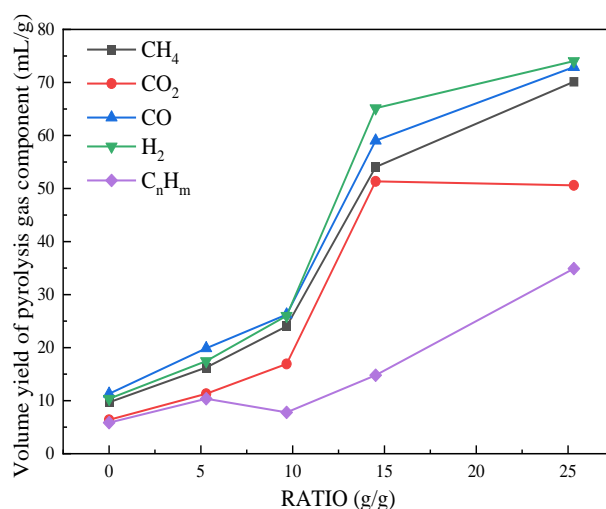


Figure 4. The effect of RATIO on pyrolysis gas components.

3.3. Composition of Tar

In the GC-MS analysis of tar, dozens of hydrocarbons have been identified. For better analysis of tar chemical components, these hydrocarbons are sorted in the order of peak area percentage content from high to low, and those components with the same molecular formula but different molecular structure are merged. Following this method, 60 distinct hydrocarbon compounds are identified and analyzed, each of which possesses a unique structure. These hydrocarbons are categorized into aliphatic compounds, aliphatic ring compounds, monocyclic aromatic hydrocarbons, polycyclic aromatic hydrocarbons, and others. Figure 5 illustrates the percentage content of these five types of tar components at different RATIOS. Obviously, the tar mainly contains monocyclic aromatic hydrocarbons, polycyclic aromatic hydrocarbons, and aliphatic compounds, the sum content of which exceeds 96%. It is also found that there is a strong correlation between tar component (including the type and content) and RATIO. Specifically, in the absence of solid heat carriers, monocyclic aromatic hydrocarbons constitute the majority of the pyrolysis tar at 54.32%, while in the cases with solid heat carrier the content of such hydrocarbons decreases to varying degree and meanwhile the proportion of polycyclic aromatic hydrocarbons increases. This indicates that with the addition of solid heat carrier, the tar secondary reactions intensify, leading to the polymerization of monobenzene ring aromatic hydrocarbons to form polycyclic aromatic hydrocarbons. In this case, the aromaticity of the tar is enhanced. For instance, at the RATIO of 9.67 g/g, there exist 33 types of monocyclic aromatic hydrocarbons in tar, accounting for 43.1% of the tar.

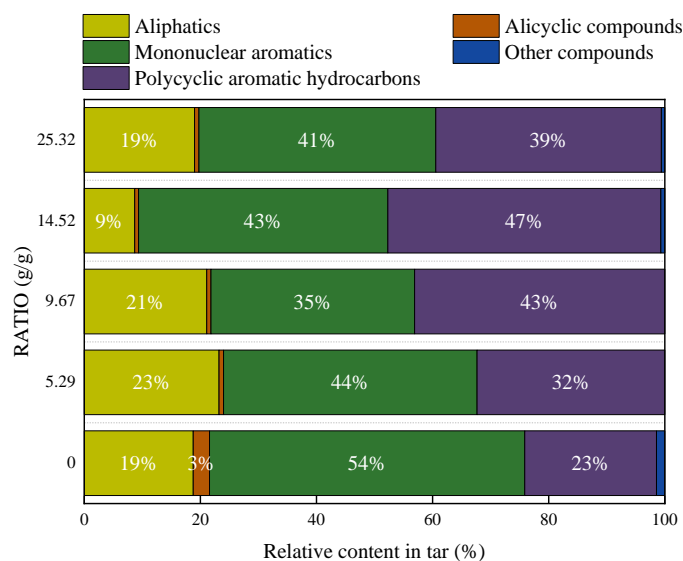


Figure 5. The effect of RATIO on chemical composition of pyrolysis tar.

To further evaluate tar quality, a detailed ion flow chromatography of the tar is given in Figure 6, with the case of the RATIO of 14.52 g/g as an example. The primary compounds identified in this tar sample include aliphatic compounds (C_{14} – C_{40} alkanes: 6.79%, alcohols: 1.44%), benzene (8.38%) and its derivatives (methyl phenol: 21.32%, phenol: 11.28%, hydrazine: 4.37%), and polycyclic aromatic hydrocarbons (naphthalene and its derivatives: 30.1%, hydrazine: 3.7%, hydrazine and its derivatives: 3.39%). Based on the tar compositions, it can be found that the tar predominantly consists of aromatic compounds, and the vast majority are aromatic hydrocarbons with two or more rings. Furthermore, the tar is also rich in low-grade phenolic compounds. Given these characteristics, this tar is apt for the extraction of phenolic chemical raw materials or for hydrogenating gasoline and other fuels, making it an excellent choice of raw materials for high-quality hydrotreating applications [34].

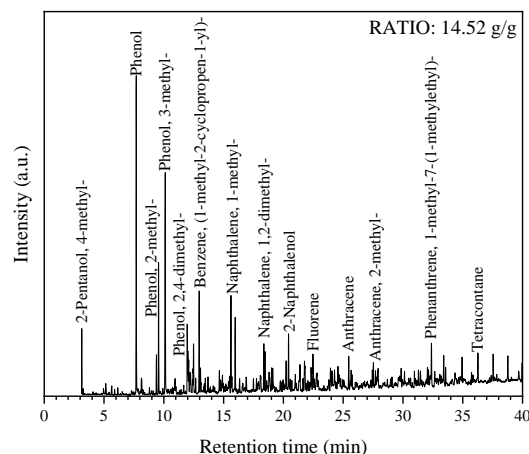


Figure 6. Gas chromatogram of pyrolysis tar at the RATIO of 14.52 g/g.

Figure 7 illustrates the fraction distribution of pyrolysis tar at different RATIOS. According to the boiling points of different fractions, the tar components can be divided into six categories: light oils (below 170 °C), phenol oils (170–210 °C), naphthalene oils (210–230 °C), washing oils (230–300 °C), anthracene oil (300–360 °C), and asphalt (above 360 °C) [35]. Generally, the fractions with a boiling point below 360 °C are collectively referred to as light components. As seen from Figure 7, without the solid heat carrier, the light component content is 30.75% and the heavy asphalt content stands at 68.75%. As the RATIO escalates, there is an increase in the light component content and a decrease in the asphalt content. This suggests that the heavy asphalt is transformed into lighter tar. Such transformation is obviously related to the aforesaid catalytic effect of solid heat carrier of SMC on heavy tar. In this transformation process, the aromatic ring structure of macromolecular asphalt breaks down into light tar with smaller aromatic ring structure, gas, and coke. At the RATIO of 14.52 g/g, the light component content seems to reach the maximum, constituting 54.67% of the tar content. Further increasing the RATIO, the light component content slightly diminishes and the asphalt content accordingly rebounds. Overall, relative to the pyrolysis tar devoid of solid heat carrier, the light component content in tar augments with RATIO, underscoring the potential benefits of solid heat carrier for enhancing tar quality.

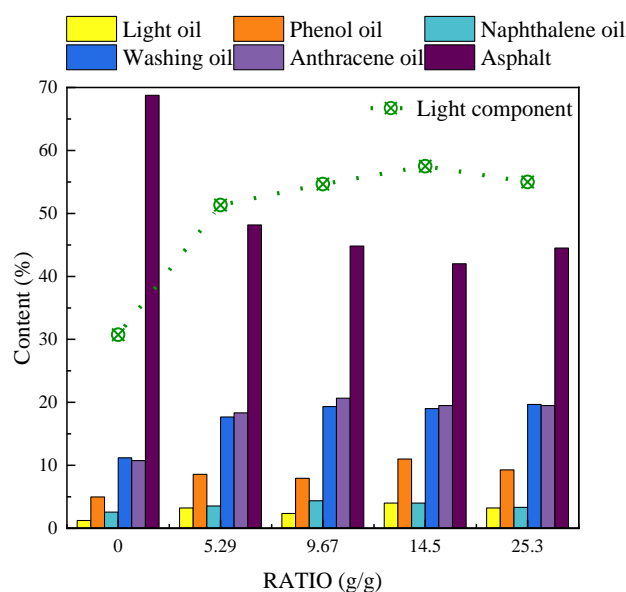


Figure 7. The effect of RATIO on fraction distribution of pyrolysis tar.

3.4. Characterization Analysis of Char

The results of porous structure and proximate analysis of pyrolysis char at different RATIOS are listed in Table 2. There seems to be a trend that with the increase of RATIO, the porous structure of char develops first and then declines. For instance, at a relatively low RATIO of 5.29 g/g, the char is characterized by a S_{BET} of 7.204 m²/g and a V_{TOT} of 0.02655 cm³/g, while the S_{BET} and V_{TOT} of the char, respectively, reduce to 3.253 m²/g of 0.02181 cm³/g at a relatively high RATIO of 25.32 g/g. In a general, the more developed porous structure of the char, the more active sites on the char surface, which can promote the secondary cracking of tar [36]. However, the secondary cracking of large tar molecules will conversely form coke to block the pores inside the char [37]. Hence, the porous structure of char is the consequence of mutual constraints among different pyrolysis reactions. In these experiments, it is evident that the negative effects of the secondary cracking reaction on the porous structure of char seems stronger at a higher RATIO. According to proximate analysis results, with the increase of RATIO, the volatile matter content of char shows a downward trend as a whole. At a RATIO of 9.67 g/g, the removal ratio of volatile matter reaches a maximum of 83.34%. These results regarding proximate analysis also seems to be attributed to the more intensified secondary cracking reaction of tar at higher RATIO, leading to more volatile matter being converted into coke.

Table 2. Porous structure and proximate analysis of char at different RATIOS.

No.	RATIO (g/g)	S_{BET} (m ² /g)	V_{TOT} (cm ³ /g)	Proximate Analysis (% ad)			
				M	V	FC	A
1	0	3.648	0.02606	0.00	11.29	77.46	11.26
2	5.29	7.204	0.02655	0.00	9.94	78.00	12.07
3	9.67	7.138	0.02675	0.00	9.97	76.67	13.36
4	14.52	3.207	0.02236	0.00	10.94	76.03	13.03
5	25.32	3.253	0.02181	0.00	9.82	77.48	12.70

Figure 8 shows the FTIR spectra of SM and chars at different RATIOS. Due to the obvious FTIR spectrum differences between SM and chars, especially in the ranges of 1750–400 cm^{−1} and 3100–2700 cm^{−1}, it is confirmed that the surface chemical properties of SM have undergone significant change in the pyrolysis process. Similarly, such a conclusion also applies to the pyrolysis process of SM at different RATIOS because of visible differences of FTIR spectra in the range of 1750–400 cm^{−1}.

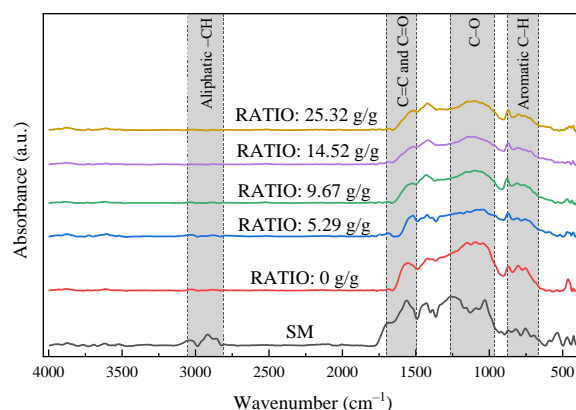


Figure 8. FTIR spectra of coal and char at different RATIOS.

To quantitatively compare the changes in surface chemical property, in this study, seven infrared structural parameters (A_{ar} , A_{al} , $\frac{H_{\text{al}}}{H_{\text{ar}}}$, $A_{1700-1500}$, $I_{1750-1500}$, $A_{900-700}$, $I_{900-700}$) are defined according to Refs. [38,39], and the peak area of each characteristic peak is obtained by piecewise curve fitting to characterize the chemical structure of organic matter

in char. A_{ar} is the absorbance integral area in the aromatic hydrogen band of the infrared spectrum (3100–3000 cm^{-1}). A_{al} is the absorbance integral area in the aliphatic hydrogen band of the infrared spectrum (3000–2700 cm^{-1}). $\frac{H_{al}}{H_{ar}}$ is the absorbance integral area ratio of aliphatic hydrogen to aromatic hydrogen, representing the degree of thermal evolution of organic matter. A smaller $\frac{H_{al}}{H_{ar}}$ indicates a higher degree of thermal evolution of char. $A_{1750-1500}$ is the absorbance integral area in the band of aromatic ring C=C double bond and C=O double bond in the infrared spectrum (1750–1500 cm^{-1}). $I_{1750-1500}$ is the relative change of char macromolecule C=C double bond, characterizing the degree of fragmentation of the char macromolecule. $A_{900-700}$ is the absorbance integral area in the band of benzene ring substitution on the infrared spectrum (900–700 cm^{-1}). $I_{900-700}$ is the relative change of benzene ring substitution in the char. The corresponding calculation results are shown in Table 3.

Table 3. FTIR spectra parameter of raw coal and char.

Sample	RATIO (g/g)	A_{ar}	A_{al}	$\frac{H_{al}}{H_{ar}}$	$A_{1750-1500}$	$I_{1750-1500}$	$A_{900-700}$	$I_{900-700}$
SM	-	88.78	231.41	2.40	1635.93	1.00	600.26	1.00
	0	11.84	18.63	1.45	688.00	0.42	905.33	1.51
	5.29	26.74	35.71	1.23	389.44	0.24	785.09	1.31
Char	9.67	8.52	11.01	1.19	447.26	0.27	810.38	1.35
	14.52	1.04	2.08	1.84	434.16	0.26	701.09	1.17
	25.32	2.42	0.84	0.32	413.93	0.25	631.08	1.05

It can be inferred that in the pyrolysis process, the benzene ring structure in coal molecules and C=O side chain in macromolecules fracture, reducing the contents of C=C and C=O on the solid surface. Compared with the case without the solid heat carrier, the intervention of the solid heat carrier reduces the value of $I_{1750-1500}$ from 0.42 to within the range of 0.24–0.27. This indicates that the solid heat carrier intensifies the fracture of macromolecular benzene ring structure and the fragmentation seems unaffected by the RATIO. At the same time, $\frac{H_{al}}{H_{ar}}$ shows a decreasing trend from 1.45 to 0.32 with RATIO. Hence, under the action of more solid heat carrier, the char undergoes a stronger thermal evolution process. Similarly, the monotonously decreasing trend of $I_{900-700}$ from 1.52 at the RATIO of 0 g/g to 1.05 at the RATIO of 25.32 g/g is due to the fact that the aromatic groups of char macromolecules have been broken.

4. Conclusions

In this study, pulverized SM with a particle size of 0–0.1 mm was pyrolyzed at 650 °C in a lab-scale fluidized bed reactor, utilizing SMC as the solid heat carrier. The influence of mass ratio of char to coal (RATIO) was investigated. Primary conclusions are drawn as follows.

- (1) As the RATIO increased, there was a rise in the yields of gas and tar but a decrease in the yield of char. Notably, at the RATIO of 14.52 g/g, the tar yield reached its peak within the range of 8.33–14.68%, accounting for 148.80–262.22% of the Gray–King analysis value.
- (2) A higher RATIO intensified the polymerization of monobenzene ring aromatic hydrocarbons, leading to a swift rise in both concentration and quantity of polycyclic aromatic hydrocarbons and thereby enhancing the aromaticity of the tar. Specifically, at the RATIO of 14.52 g/g, the tar mainly consisted of aromatic compounds, characterized with two or more aromatic rings and enriched in low-grade phenolic components, such as naphthalene and its derivatives (30.1%) and methyl phenol (21.32%). Moreover, the presence of solid heat carrier of char improved tar quality due to more light components in the tar.

- (3) Solid heat carrier promotes the release of volatile matter by intensifying the primary pyrolysis reaction, while suppressing it by enhancing the secondary cracking of tar. The removal ratio of volatile matter reaches a maximum of 83.34% at the RATIO of 9.67 g/g. The addition of solid heat carrier fractures the macromolecular benzene ring structure and the aromatic groups of char macromolecules, enhancing the thermal evolution process of char.

Author Contributions: Conceptualization, X.Q. and Z.Z.; Methodology, X.L. and R.C.; Formal analysis, X.L. and R.C.; Investigation, X.L. and R.C.; Data curation, X.L.; Writing—original draft, X.L.; Writing—review & editing, X.Q.; Supervision, X.Q., Z.Z. and X.W.; Project administration, X.Q., Z.Z. and X.W.; Funding acquisition, X.Q. All authors have read and agreed to the published version of the manuscript.

Funding: This work was supported by the Strategic Priority Research Program of the Chinese Academy of Sciences (No. XDA29020600).

Data Availability Statement: Data is contained within the article.

Conflicts of Interest: The authors declare no conflict of interest.

References

- Xu, S.; Zeng, X.; Han, Z.; Cheng, J.; Wu, R.; Chen, Z.; Masek, O.; Fang, X.; Xu, G. Quick pyrolysis of a massive coal sample via rapid infrared heating. *Appl. Energy* **2019**, *242*, 732–740. [\[CrossRef\]](#)
- Du, Z.; Li, W. The Catalytic Effect from Alkaline Elements on the Tar-Rich Coal Pyrolysis. *Catalysts* **2022**, *12*, 376. [\[CrossRef\]](#)
- Han, J.; Wang, X.; Yue, J.; Gao, S.; Xu, G. Catalytic upgrading of coal pyrolysis tar over char-based catalysts. *Fuel Process. Technol.* **2014**, *122*, 98–106. [\[CrossRef\]](#)
- Jin, X.; Li, X.; Kong, J.; Xie, W.; Wang, M.; Wang, J.; Bao, W.; Chang, L. Insights into coke formation during thermal reaction of six different distillates from the same coal tar. *Fuel Process. Technol.* **2021**, *211*, 106592. [\[CrossRef\]](#)
- Fan, Y.; Zhang, S.; Li, X.; Xu, J.; Wu, Z.; Yang, B. Process intensification on suspension pyrolysis of ultra-fine low-rank pulverized coal via conveyor bed on pilot scale: Distribution and characteristics of products. *Fuel* **2021**, *286*, 119341. [\[CrossRef\]](#)
- Liang, P.; Wang, Z.; Bi, J. Process characteristics investigation of simulated circulating fluidized bed combustion combined with coal pyrolysis. *Fuel Process. Technol.* **2007**, *88*, 23–28. [\[CrossRef\]](#)
- Chen, X.; Zhao, Y.; Liu, L.; Zhang, L.; Zhang, Z.; Qiu, P. Evaluation of chemical structure, pyrolysis reactivity and gaseous products of Shenmu coal of different particle sizes. *J. Anal. Appl. Pyrolysis* **2018**, *130*, 294–304. [\[CrossRef\]](#)
- Zhu, W.; Song, W.; Lin, W. Effect of the Coal Particle Size on Pyrolysis and Char Reactivity for Two Types of Coal and Demineralized Coal. *Energy Fuels* **2008**, *22*, 2482–2487. [\[CrossRef\]](#)
- Zhou, Q.; Liu, Q.; Shi, L.; Yan, Y.; Liu, Z. Behaviors of coking and radicals during reaction of volatiles generated from fixed-bed pyrolysis of a lignite and a subbituminous coal. *Fuel Process. Technol.* **2017**, *161*, 304–310. [\[CrossRef\]](#)
- Hao, S.; Zhang, L.; Jia, Y. Synergistic effect of blast furnace slag on the pyrolysis process of oil-rich coal, tar product distribution and kinetic analysis. *Energy Sources Part A-Recovery Util. Environ. Eff.* **2021**, 1–14. [\[CrossRef\]](#)
- Duan, W.; Yu, Q.; Xie, H.; Qin, Q. Pyrolysis of coal by solid heat carrier-experimental study and kinetic modeling. *Energy* **2017**, *135*, 317–326. [\[CrossRef\]](#)
- Liu, Z.; Guo, X.; Shi, L.; He, W.; Wu, J.; Liu, Q.; Liu, J. Reaction of volatiles—A crucial step in pyrolysis of coals. *Fuel* **2015**, *154*, 361–369. [\[CrossRef\]](#)
- Fushimi, C.; Okuyama, S.; Kobayashi, M.; Koyama, M.; Tanimura, H.; Fukushima, H.; Thangavel, S.; Matsuoka, K. Pyrolysis of low-rank coal with heat-carrying particles in a downer reactor. *Fuel Process. Technol.* **2017**, *167*, 136–145. [\[CrossRef\]](#)
- Liang, P.; Wang, Z.; Dong, Y.; Bi, J. Experimental investigation of solid heat carrier pyrolysis of Huainan coal. *J. Fuel Chem. Technol.* **2005**, *33*, 257–262.
- Xue, F.; Li, D.; Guo, Y.; Liu, X.; Zhang, X.; Zhou, Q.; Ma, B. Technical Progress and the Prospect of Low-Rank Coal Pyrolysis in China. *Energy Technol.* **2017**, *5*, 1897–1907. [\[CrossRef\]](#)
- Qu, X.; Liang, P.; Wang, Z.; Zhang, R.; Sun, D.; Gong, X.; Gan, Z.; Bi, J. Pilot Development of a Polygeneration Process of Circulating Fluidized Bed Combustion combined with Coal Pyrolysis. *Chem. Eng. Technol.* **2011**, *34*, 61–68. [\[CrossRef\]](#)
- Cui, Y. Research status and prospects on pyrolysis technologies of the pulverized coal. *Energy Chem. Ind.* **2018**, *39*, 33–38.
- Silvestre, W.P.; Pauletti, G.F.; Godinho, M.; Baldasso, C. Fodder radish seed cake pyrolysis for bio-oil production in a rotary kiln reactor. *Chem. Eng. Process. Process Intensif.* **2018**, *124*, 235–244. [\[CrossRef\]](#)
- Daugaard, T.J.; Dalluge, D.L.; Brown, R.C.; Wright, M.M. Effect of thermophysical properties of heat carriers on performance of a laboratory-scale auger pyrolyzer. *Fuel Process. Technol.* **2018**, *176*, 182–189. [\[CrossRef\]](#)
- Qu, X.; Zhang, R.; Sun, D.; Bi, J. Experiment study on pyrolysis of Huolinhe lignite with solid heat carrier. *J. Fuel Chem. Technol.* **2011**, *35*, 85–89.

21. Zhang, Y.; Liang, P.; Zhu, J.; Yu, J.; Qin, X. Secondary Catalytic Reaction of Circulating Ash on the Primary Volatiles of Coal Pyrolysis. *J. Energy Eng.* **2017**, *143*, 04017021. [\[CrossRef\]](#)
22. Li, T.; Du, T.; Shen, Y.; Yan, L.; Kong, J.; Wang, M.; Wang, J.; Chang, L.; Bao, W. Effect of char powder on gaseous tar reaction during low-rank coal pyrolysis. *J. Fuel Chem. Technol.* **2021**, *49*, 626–633. [\[CrossRef\]](#)
23. Li, X.H.; Li, B.F.; Fu, D.Q.; Feng, J.; Li, W.Y. The interaction between the char solid heat carrier and the volatiles during low-rank coal pyrolysis. *J. Anal. Appl. Pyrolysis* **2018**, *136*, 160–168. [\[CrossRef\]](#)
24. Lyu, Q.; Yu, K.; Zhu, Z.; Meng, G. Pilot plant research on fast pyrolysis of coal in circulating fluidized bed with hot char carrier. *J. China Coal Soc.* **2012**, *37*, 1591–1595.
25. Guo, M.; Bi, J. Experimental study on Fugu coal pyrolysis with solid heat carrier. *Coal Convers.* **2016**, *39*, 26–30, 61.
26. Pan, D.F.; Qu, X.; Bi, J.C. Effect of gasified semi-coke on coal pyrolysis in the poly-generation of CFB gasification combined with coal pyrolysis. *J. Anal. Appl. Pyrolysis* **2017**, *127*, 461–467. [\[CrossRef\]](#)
27. Li, X.H.; Ma, J.S.; Li, L.L.; Li, B.F.; Feng, J.; Turmel, W.; Li, W.Y. Semi-coke as solid heat carrier for low-temperature coal tar upgrading. *Fuel Process. Technol.* **2016**, *143*, 79–85. [\[CrossRef\]](#)
28. Zhang, X.; Wang, L.; Pei, X.; Wang, Y.; Zhou, Q. Research progress and key technology of improving coal tar yield and quality by coal pyrolysis. *Coal Sci. Technol.* **2019**, *47*, 227–233.
29. Quan, S.; Shi, L.; Zhou, B.; Liu, Z.; Liu, Q. Study of temperature variation of walnut shell and solid heat carrier and their effect on primary pyrolysis and volatiles reaction. *Fuel* **2021**, *292*, 120290. [\[CrossRef\]](#)
30. ASTM D2887-01a; Standard Test Method for Boiling Range Distribution of Petroleum Fractions by Gas Chromatography. ASTM International: West Conshohocken, PA, USA, 2010.
31. SH/T 0558-95; Method for Determination of Boiling Range Distribution of Petroleum Fractions (Gas Chromatography). China Petrochemical Corporation: Beijing, China, 1994.
32. Jiang, Y.; Zong, P.; Ming, X.; Wei, H.; Zhang, X.; Bao, Y.; Tian, B.; Tian, Y.; Qiao, Y. High-temperature fast pyrolysis of coal: An applied basic research using thermal gravimetric analyzer and the downer reactor. *Energy* **2021**, *223*, 119977. [\[CrossRef\]](#)
33. Jin, L.; Bai, X.; Li, Y.; Dong, C.; Hu, H.; Li, X. In-situ catalytic upgrading of coal pyrolysis tar on carbon-based catalyst in a fixed-bed reactor. *Fuel Process. Technol.* **2016**, *147*, 41–46. [\[CrossRef\]](#)
34. Liu, F.; Wang, L.; Yang, W.; Li, Z.; Zhu, Y. Study on deep-processing technology of medium and low temperature coal tar and analysis of its market prospect. *Mod. Chem. Ind.* **2012**, *32*, 7–11.
35. Li, X.; Jin, X.; Wang, M.; Yu, Y.; Kong, J.; Xie, W.; Wang, J.; Chang, L.; Bao, W. Effect of volatiles' reaction on coking of tar during pyrolysis of Naomaohu coal in a downer-bed reactor. *Fuel Process. Technol.* **2021**, *212*, 106623. [\[CrossRef\]](#)
36. Xing, X.; Zhao, H.; Zhou, L.; Wang, Y.; Chen, H.; Gao, Y.; Wang, Y.; Zhu, Y. Pyrolysis kinetics, thermodynamics of PTA sludge and product characterization of cyclic in-situ catalytic pyrolysis by using recycled char as a catalyst. *Energy* **2022**, *251*, 123821. [\[CrossRef\]](#)
37. Zhang, W.; He, Y.; Wang, Y.; Li, G.; Chen, J.; Zhu, Y. Comprehensive investigation on the gasification reactivity of pyrolysis residue derived from Ca-rich petrochemical sludge: Roles of microstructure characteristics and calcium evolution. *Energy Convers. Manag.* **2022**, *253*, 115150. [\[CrossRef\]](#)
38. Solomon, P.R.; Carangelo, R.M. FT-i.r. analysis of coal: 2. Aliphatic and aromatic hydrogen concentration. *Fuel* **1988**, *67*, 949–959. [\[CrossRef\]](#)
39. He, X.; Liu, X.; Nie, B.; Song, D. FTIR and Raman spectroscopy characterization of functional groups in various rank coals. *Fuel* **2017**, *206*, 555–563. [\[CrossRef\]](#)

Disclaimer/Publisher's Note: The statements, opinions and data contained in all publications are solely those of the individual author(s) and contributor(s) and not of MDPI and/or the editor(s). MDPI and/or the editor(s) disclaim responsibility for any injury to people or property resulting from any ideas, methods, instructions or products referred to in the content.